



HAL
open science

Surface current and eddy-current 3D computation using boundary integral equations techniques

Laurent Krähenbühl

► **To cite this version:**

Laurent Krähenbühl. Surface current and eddy-current 3D computation using boundary integral equations techniques. 3th IGTE, Sep 1988, Graz, Austria. pp.40-50. hal-01745580

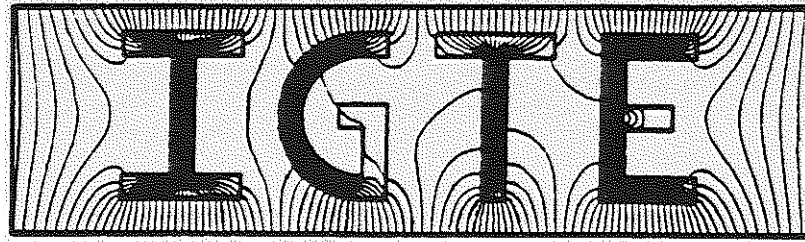
HAL Id: hal-01745580

<https://hal.science/hal-01745580>

Submitted on 3 Apr 2018

HAL is a multi-disciplinary open access archive for the deposit and dissemination of scientific research documents, whether they are published or not. The documents may come from teaching and research institutions in France or abroad, or from public or private research centers.

L'archive ouverte pluridisciplinaire **HAL**, est destinée au dépôt et à la diffusion de documents scientifiques de niveau recherche, publiés ou non, émanant des établissements d'enseignement et de recherche français ou étrangers, des laboratoires publics ou privés.



INSTITUT FÜR
GRUNDLAGEN UND THEORIE DER ELEKTROTECHNIK
TECHNISCHE UNIVERSITÄT GRAZ

3rd INTERNATIONAL
IGTE SYMPOSIUM

1988

NUMERICAL FIELD CALCULATION
IN ELECTRICAL ENGINEERING

PROCEEDINGS

SEPTEMBER 27./28. 1988

GRAZ, AUSTRIA

Surface current and eddy-current 3D computation using boundary integral equations techniques

0. Introduction

0.1. The problem of *eddy-currents* calculation.

In many industrial applications, the exact computation of the eddy-current distribution is a major step of CAD operation. This can be found in electromagnetic steel heating, non-destructive testing or electromagnetic compatibility. In a research domain this exact computation often allows to explain some phenomena or some behaviour of a system. In some applications, when no simplification can be found in the geometry, the computation has to be a 3D computation.

The three usual electromagnetic field computation methods can be used: *finite difference*, *finite elements* and *boundary integral equations*.

Finite difference and *finite elements* methods require a volumic mesh for a 3D solution. In addition of the difficulty to mesh an exterior domain (because of the limit at infinite), these methods make appear some problems when the frequency of the eddy-currents becomes high enough to give a very thin skin depth: a well suited mesh leads to a prohibitive number of nodes.

Instead of that, BIE method appears as performant when the skin depth becomes small: in this case any approximation which relates the *volumic* eddy-currents contribution to that of a *surfacic* quantity can be accepted.

0.2. The content of this paper.

This paper is devoted to our most recent works in the domain of the high frequency eddy-currents computation. We have in fact define two classes of frequencies: *high* frequency and *very high* (also called *infinite*) frequency, this one beeing a limit case of the previous one:

- the *very high* or *infinite frequency* formulation has been presented in previous papers since 1981 ([2], [3], [4], [5]). This formulation is very easy to built in, and gives approximate results with a low computing time.

However the physical meaning of the results and the range of frequency in what this model could be used were not easy to understand: we give in this paper a new idea of that, using the results of the *high frequency* formulation:

- the *high frequency* formulation takes into account the exponential decay of the magnetic field inside the conducting materials and the penetration of the induction field. This model has been validated by comparison with analytical calculations.

Before to present in detail and discuss these problems, we will quickly remind the BIE formulation used in our package PHI3D ([3], [7]).

0.3. The boundary integral formulation used in PHI3D [3].

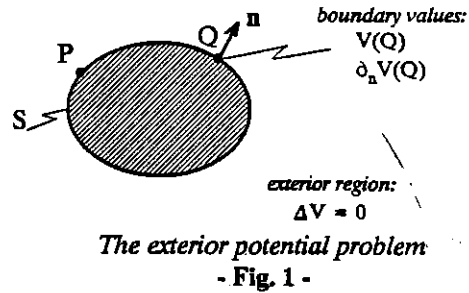
Consider the *exterior region* on Fig. 1. The Laplace's equation valid in this whole region is equivalent to the BIE:

$$c.V(P) = - \int_S [V(Q) \cdot \partial_n G_p(Q) - \partial_n V(Q) \cdot G_p(Q)] \cdot ds \quad (0)$$

expressed on the whole surface S.

According to the type of problem, V is known a priori and $\partial_n V$ is to be found, or vice versa, or both functions are unknown. In that case, one has to find a complementary relation between these boundary values.

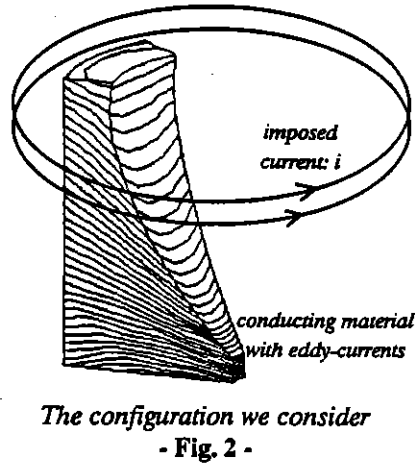
For solving our eddy-currents problem with this BIE method, we will have a *scalar potential V* appear and also its values V and $\partial_n V$ on the surface S.



0.4. Studied configuration and notations.

0.4.1. Configuration.

The studied configuration is shown on Fig. 2: a given inductor current i at the frequency f causes eddy-currents into the conductor piece which surface is S.



0.4.2. The problem.

The problem is to determine the field **H** in the air surrounding the conductor as the sum of:

- the field H_0 due to the known current i (*inductor field*);
- the response field H_i due to the eddy-currents (*induced field*).

This induced field derivates (in the air-region) from a scalar potential V which Laplacian is null: nothing remains but to find a boundary condition to take into account these eddy-currents: we will propose successively two, corresponding to the *infinite frequency* and *high frequency* models.

0.4.3. Notations.

The following conventions and notations are used in this paper:

- the *vectors* are printed using the bold types: **H**, **B**, **j**, etc.
- the *modulus* using the normal types: H, B, j, etc.
- the *differential operators* are:

$\partial_n f$:	derivative of f in the direction n
grad	is the ∇ operator
div	is the $\nabla \cdot$ operator
lap	is the ∇^2 or Δ operator
- the index S indicates a surface restriction of these operators: grad_S , div_S , lap_S , etc.

1. The *infinite frequency* formulation.

1.1. Hypothesis and method.

In that limit case, the eddy-currents are supposed to be made of a *surface current density* working as a perfect magnetic screen: the field is null in the conducting volume; so the boundary condition is:

$$\mathbf{H} \cdot \mathbf{n} = 0 \quad \text{on the exterior side of } S. \quad (1)$$

This exterior field problem, expressed in terms of potential:

$$\begin{aligned} \text{lap } V &= 0 && \text{Laplace's equation into the air-region} \\ \partial_n V &= H_0 \cdot \mathbf{n} && \text{Neuman's boundary condition} \end{aligned} \quad (2)$$

with:

$$\begin{aligned} H_0 &&& \text{primary field (Biot and Savart law)} \\ H_1 &&& \text{induced field (eddy-currents)} \\ \mathbf{H} &= H_0 + H_1 && \text{total field (= 0 in the conductor)} \\ V &&& \text{scalar potential of } H_1 \end{aligned} \quad (3)$$

is easily solved using the Boundary Integral Equation Method.

1.2. Determination of the eddy-currents.

The BIEM allows to compute the field values on any point *outside of* or *on* the conducting piece. It would be also useful to be able to draw the *current lines* on the surface of the conductor and to compute the *current densities*.

1.2.1. General properties of the surface current densities.

We will first remind two basic properties of the *surface current density* \mathbf{K} [1]:

(1) On a detached conducting surface, \mathbf{K} derives from a *current function* F :

$$\mathbf{K} = - (\mathbf{n} \times \text{grad}_S F) \quad (4)$$

The isovalues of F are the *current lines*, and the difference $F(P') - F(P)$ represents the current flowing between points P and P' .

(2) The induction field is *discontinuous* through the current density \mathbf{K} :

$$\mathbf{B}_+ - \mathbf{B}_- = - \mu_0 \cdot (\mathbf{n} \times \mathbf{K}) \quad (5)$$

This discontinuity is tangential to S and orthogonal to \mathbf{K} .

Note that the field \mathbf{H} and the surface current density \mathbf{K} are expressed in the same unit. In like a manner, F is expressed in [A] like a magnetic potential.

1.2.2. Particular case: the infinite frequency.

In that case, B_+ is assumed to be zero in equation (5). One has on the air-side of the conductor:

$$B_+ = -\mu_0 \cdot (n \times K) \quad \Leftrightarrow \quad K = n \times H_+ \quad (6)$$

As a result, the *surface current density* is equal (in modulus) to the *field* on S. It will be determined from the BIE solution with:

$$H_+ = H_{0,tg} - \text{grad}_S V \quad (7)$$

We have now to find the *current function* F which allows the draw of the current lines.

Equation (4) compared to (6) gives:

$$-\text{grad}_S F = H_+ \quad (8)$$

It means that the total field H derivates on S from the *current function* F which is then confused with the *total scalar magnetic potential*: one has:

$$F = V + V_0 \quad (9)$$

where V_0 is the scalar potential of the inductor field H_0 . Although this field is known, the computation of the associated potential is not trivial.

1.2.3. Computation of the potential of the primary field.

Let us consider a field H_0 on a surface S. We search after a potential V_0 on S as:

$$-\text{grad}_S V_0 = H_{0,tg} \quad (10)$$

With this end in view, we use once more the discretization of S into finite elements. V_0 will be also discretized and its nodal values adjusted to minimize the quadratic difference:

$$\int_S (H_{0,tg} + \text{grad}_S V_0)^2 \cdot ds$$

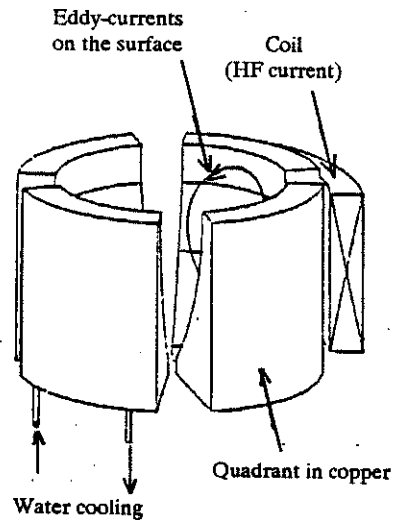
To remove the undefined constant, a value is arbitrary given on a particular node. The matrix of the obtained linear system is diagonal, symmetric and positive.

With the *infinite frequency* model, the eddy-current problem is reduced to an exterior potential problem with Neuman's boundary conditions. The BIEM is well suited to solve it. We have shown how to obtain the current densities and the current lines from this BIE solution. We will now give some examples.

1.3. Examples.

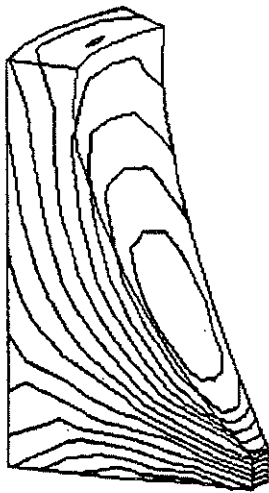
1.3.1. The inevitable cold crucible.

This example was previously explained and published on several occasions ([3], [4], [5] for example). We are today in a position to show some physical meaning values on its surface (Fig. 3).

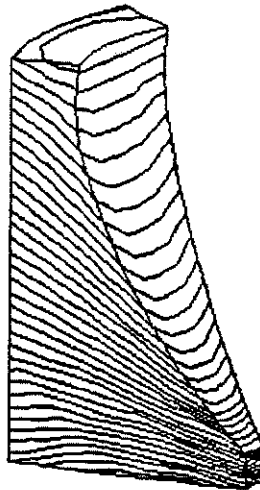


(a) Principle of the cold crucible

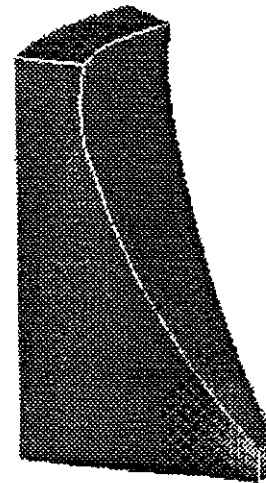
- Fig. 3 -
The cold crucible



(b) Isovalues of potential V without physical meaning

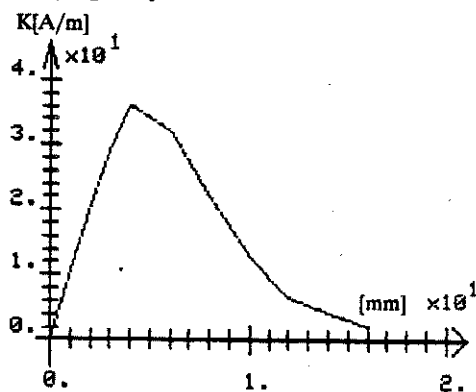
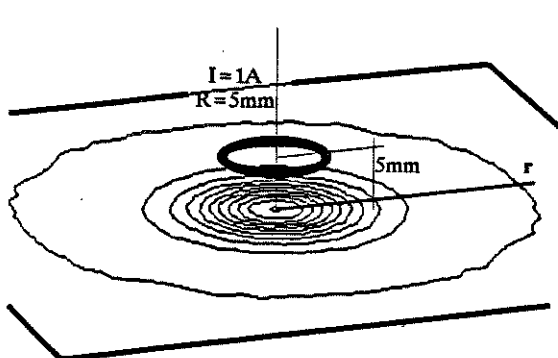


(c) Isovalues of the current function F equivalent to the current lines



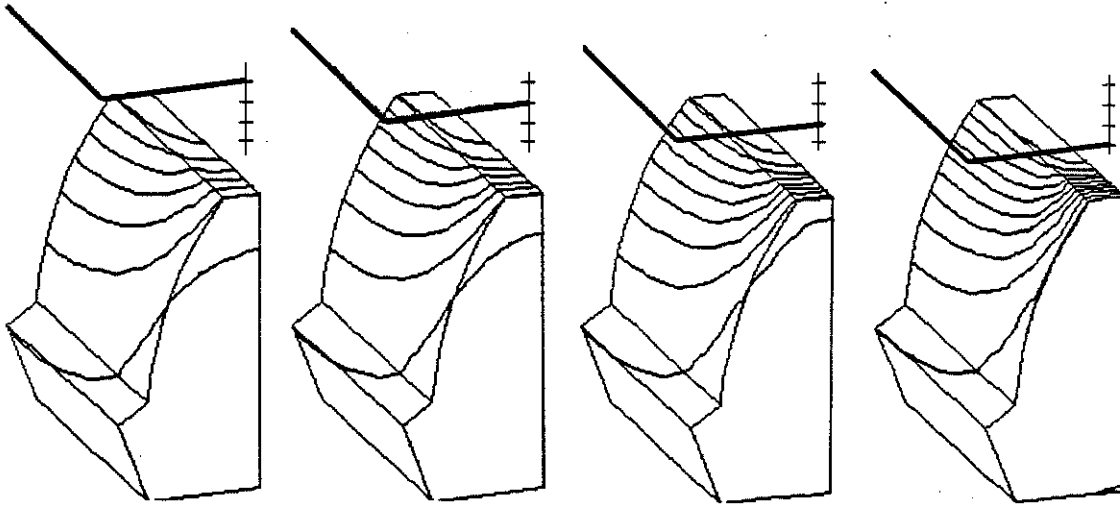
(d) Modulus of the field H equivalent to the current

1.3.2. Dodd's test-problem (see §2.4) computed in infinite frequency.



Current lines (a) and current density as a function of r (b)

- Fig. 4 -



*Eddy-current lines on a gear-wheel (steel hardening)
for different positions of the inductor current-loop.
Computed with two symmetries.*

- Fig. 5 -

2. The *high frequency* formulation.

2.1. Introduction.

The *infinite frequency* model is a good model: every body knows that either at very high frequency or during the first instants of a transient phenomenon the magnetic field is unable to penetrate inside a conducting material.

On the other side, this model does not allow to reach the volumic distribution of the eddy-currents, that always exists even if the frequency is very high. Besides the *infinite frequency* model ignores the *dephasing* phenomena: if we look at the Maxwell's equations, it can be seen that the current density at the surface of the piece is not in phase with the tangential component of the field. It also appears as difficult to compute something like a complex power or a complex impedance.

The development of the *high frequency* model answers to these questions: it takes into account the variations of the physical quantities with the frequency and makes the *infinite frequency model* appear as only a limit.

2.2. Analytical solution for a constant tangential field.

In this section, we will first remind the regular exponential solution for eddy-currents, then deduce of it a physical interpretation of the *infinite frequency* model. In §2.3., we will refine this analytical solution to get the *high frequency* boundary condition.

2.2.1. Hypothesis and solution.

The field H is supposed to be tangential and constant on a little area on S . The eddy-currents are supposed to flow parallel to it.

The Maxwell's equations:

$$\begin{aligned} \text{rot} H &= j \\ \text{rot} j &= \sigma \mu \partial_t H \end{aligned} \quad (11)$$

written for a sinusoidal mode:

$$\partial_t H = j\omega H \quad (12)$$

leads to the well known exponential solution inside the metal:

$$\begin{aligned} H(z) &= H_s \cdot \exp[-(j+1)z/\delta] \\ j(z) &= j_s \cdot \exp[-(1+j)z/\delta] \end{aligned} \quad (13)$$

with:

$$\begin{aligned} j_s &= -[(1+j)/\delta] \cdot \mathbf{n} \times H_s \\ \delta &= (2/\sigma\omega\mu_0\mu)^{1/2} \text{ skin depth} \end{aligned} \quad (14)$$

2.2.2. Equivalent surface current density.

The *surface* current density equivalent to the *volume* density $j(z)$ is:

$$\begin{aligned} K_{eq} &= \int_0^{\infty} j(z) \cdot dz \\ &= \mathbf{n} \times H_s \cdot \underbrace{[-(1+j)/\delta \cdot \int_0^{\infty} \exp[-(1+j)z/\delta] \cdot dz]}_{= 1} \end{aligned} \quad (15)$$

$$\text{then:} \quad K_{eq} = \mathbf{n} \times H_s \quad (16)$$

This expression, compared with (6) allows to explain physically the results of the *infinite frequency* formulation: K is the integral value of j perpendicularly to the surface. It is *in phase* with the field: that won't prevent (after resolution) from restoring the solution with its dephasing.

What to change for taking into account a z -component of the field, or a local variation of it? We will show that these two phenomena are linked.

2.3. The *high frequency* solution.

2.3.1. Boundary condition with $H_z \neq 0$

Maintaining the other hypothesis (in particular $j \cdot n = 0$), H_z appears exclusively in the third component of $\text{rot } j$:

$$\partial_x j_y - \partial_y j_x = -2j/\delta^2 \cdot H_z \quad (17)$$

The penetration of the field is then linked to the local variations of the current, then also to the variations of the tangential field. one obtains the *high frequency* boundary condition:

$$H_t \cdot n = (1-j)/2 \cdot \delta \mu_r \cdot \text{div}_s H \quad (18)$$

The right-hand term was null for the *infinite frequency* boundary condition (2). Because of the delta factor, it decreases as the square root of the frequency.

2.3.2. Resolution with both *integral* and *variational* methods.

As we did in §1.1., we separate the field in two parts:

$$H = H_0 - \text{grad}_s V$$

what leads to the system:

$$\begin{array}{l} \text{lap} V = 0 \\ \partial_n V = H_0 \cdot n + (1-j)/2 \cdot \delta \mu_r \cdot (\text{div}_s H_0 - \text{lap}_s V) \end{array} \quad \begin{array}{l} \text{Laplace's eq.} \\ \text{Boundary cond.} \end{array} \quad (18)$$

infinite freq. *correction for lower freq.*

This boundary condition links $\partial_n V$ and V through the medium of the differential operator lap_s . We solve *on the surface* using the *variational* method:

$$\text{lap}_s V = f \quad \Leftrightarrow \quad \text{minimize:} \quad \int_S [1/2 \cdot \text{grad}_s V + f \cdot V]^2 \cdot ds \quad (19)$$

and simultaneously *in the space* using the BIEM.

We take note that the expressions of the equivalent current and total potential:

$$\begin{array}{l} K_{\text{eq}} = H_{s,ig} = H_{0,ig} - \text{grad}_s V \\ F = V + V_0 \end{array} \quad (20)$$

continue to be valid. The same procedure will be used to compute it and to draw the current lines.

2.3.3. Power.

The *power density* on S will be for example computed from the *Pointing vector* ExH :

$$p = (\text{ExH}) \cdot (-n) = H_{s,ig}^2 \cdot (1+j)/\delta \sigma \quad (21)$$

The total *active power* wasted by the eddy-currents in the conducting piece is:

$$P = 1/\delta \sigma \cdot \int_S H_{s,ig}^2 \cdot ds \quad (22)$$

It is equal to the *reactive power* in the conductor and will be easily computed from the surface solution. The reactive power *in the air* surrounding the conductor is not include in this term.

2.4. Validation.

As a validation, we propose a comparison with the analytical results of Dodd [6].

2.4.1. Test configuration.

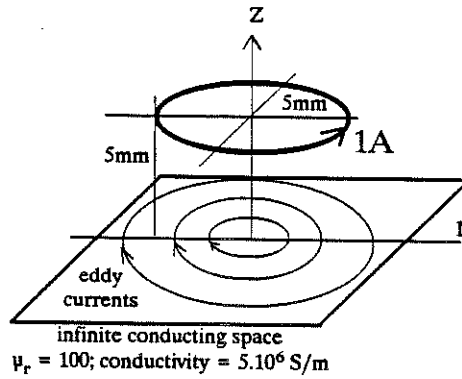
We consider a circular current in front of a half-infinite conducting space (Fig. 6). The *analytical solution* is proposed by Dodd [6].

In particular, one can calculate for each frequency the *normal field* H_z and the *tangential field* H_r (equivalent in modulus to the surface current K) on the surface of the conducting space. These values depend only on the *frequency* f and the *radius* r ; they have been tabulated by M. Mayos (IRSID).

2.4.2. Comparative results.

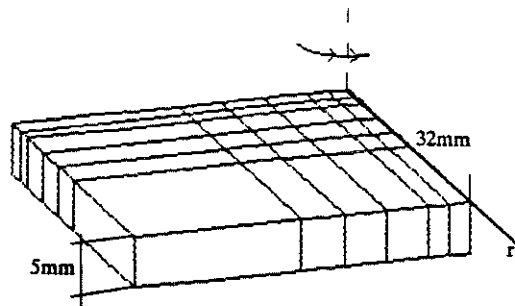
For the 3D computation, we have used a geometrically finite conductor; its dimensions and the surface-mesh are presented on Fig. 7. The results for the frequency range 1kHz ... 10MHz are presented on Fig. 8 to 10.

In a general point of view, they are excellent, but they call for some comments.



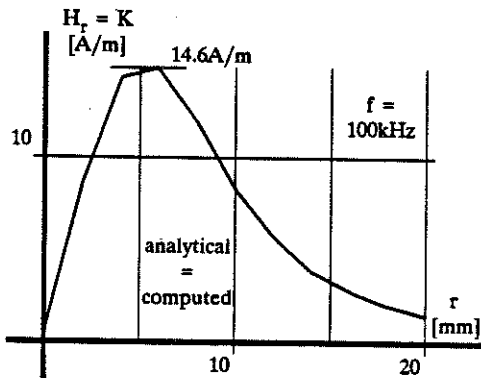
The test-problem of Dodd

- Fig. 6 -

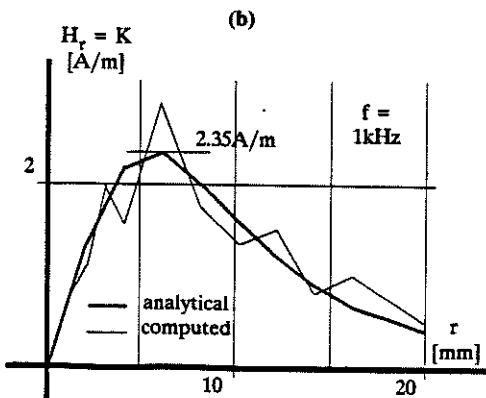


The mesh for the 3D computation

- Fig. 7 -



(a)



(b)

Current density as a function of r
(a) $f = 100\text{kHz}$ - (b) $f = 1\text{kHz}$

- Fig. 8 -

2.4.3. Error on the current density.

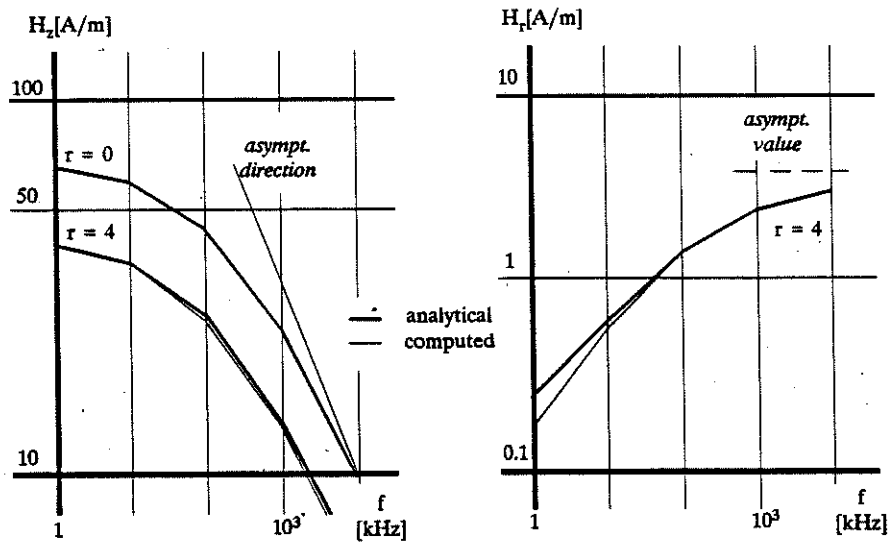
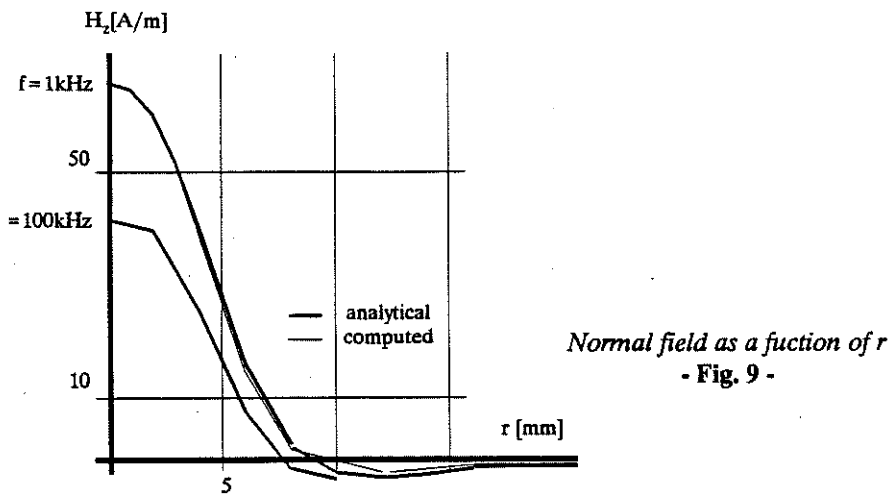
For the lower frequencies, some oscillations appear on the H_r curves (Fig. 8b). This phenomenon does not exist for the normal values of H_z , which are perfect.

By the fact, the question is *not* a global degradation of the solution. Remine eq. 20 used to compute the tangential field: for the lower frequencies, the term $H_{0,ig}$ (which does not depend on f) get balanced by the gradient of potential.

The relative error on V is very little; the corresponding error on its gradient is bigger because of the numerical derivative ($< 4\%$) and does not depend on f . The relative error on H depends on the relative values of H_z and $\text{grad}_s V$ and varies between 2% and 25%.

2.4.4. The normal field and its asymptotic values.

The results are so good that we could be afraid to be outside of the interesting frequency range. The Fig. 8 proves the contrary: two asymptotes appear, respectively for the lower frequency (H_z get constant; the limit is the static value) and for the higher (asymptotic direction in $f^{1/2}$). The *high frequency* formulation effectively allows the description of this graduated transition.



Normal field and current as functions of the frequency (Log-Log)
 - Fig. 10 -

3. Conclusion

This *high frequency* formulation has probably a fine future, in particular for the Non Destructive Testing simulations. The validation presented in this paper is at the moment beeing completed with axisymmetrical cases, comparisons with FEM techniques and so on. The research works on, to be able to compute the electrical quantities as complex impedances across an NDT-pick-up. For other applications, we are looking at the similar problem of the *high frequency conduction*.

REFERENCES

- [1] **E. Durand** *Magnétostatique* Masson et Cie, Paris, 1968
- [2] **B. Ancelle, A. Nicolas and J.C. Sabonnadière**
A boundary integral equation method for high frequency eddy currents
IEEE T-MAG Nov 81 2568-2570
- [3] **L. Krähenbühl, A. Nicolas and L. Nicolas**
A graphic interactive package for BIE
IEEE T-MAG 21/6 Nov 85
- [4] **L. Krähenbühl, A. Nicolas and L. Nicolas**
PHI3D: a graphic interactive package for 3D fields computation
Proc. of the second BETECH conference, MIT, USA, june 86
- [5] **A. Nicolas** *3D eddy current solution by BIE techniques*
IEEE T-MAG 24/1 Jan 88 130-133
- [6] **C.V. Dodd and W.E. Deeds**
Analytical solutions to eddy current probe-coil problems
1968 Journal of appl. phys. Vol 39/6
- [7] **D. Muller and L. Nicolas**
3D Post-processing for the BIEM: the example of the PHI3D package
IEEE T-MAG 24/1 Jan 88 381-384

We would like to thank M. MAYOS (IRSID, France) for the analytical results of §2.4.